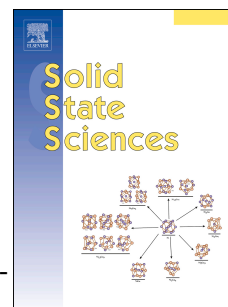# Accepted Manuscript

Versatility of copper(II) coordination compounds with 2,3-bis(2-pyridyl)pyrazine mediated by temperature, solvents and anions choice

Elena Melnic, Victor Ch Kravtsov, Karl Krämer, Jan van Leusen, Silvio Decurtins, Shi-Xia Liu, Paul Kögerler, Svetlana G. Baca

Versatility of copper(II) coordination compounds with 2,3-bis(2-pyridyl)pyrazine mediated by temperature, solvents and anions choice

Elena Melnic[a], Victor Ch. Kravtsov[*a], Karl Krämer[b], Jan van Leusen[c], Silvio Decurtinsb[2], Shi-Xia Liu[b], Paul Kögerler[c], Svetlana G. Baca[*a]

[a]Institute of Applied Physics, Academiei str. 5, MD2028 Chisinau, R. Moldova
[b]Department of Chemistry and Biochemistry, University of Bern, Freiestrasse 3, CH-3012 Bern, Switzerland
[c]Institute of Inorganic Chemistry, RWTH Aachen University, Landoltweg 1, 52074 Aachen, Germany

*Corresponding Authors: sbaca_md@yahoo.com; kravtsov@phys.asm.md

Abstract

Tuning reaction temperatures as well as the variation in starting copper salts and solvents led to the formation of a new series of Cu(II) coordination compounds with 2,3-bis(2-pyridyl)pyrazine (dpp): a mononuclear $[Cu(acac)(dpp)(NO_3)]$ (**1**) complex, two dinuclear $[Cu_2(acac)_2(dpp)(NO_3)(H_2O)]NO_3$ (**2**) and $[Cu_2(Hdpp)_2(ox)(Cl)_2(H_2O)_2]Cl_2 \cdot 6(H_2O)$ (**4**) complexes, and four coordination polymers $\{[Cu_4(dpp)_2(ox)(Cl)_6]\}_n$ (**3**),

{[Cu$_4$(dpp)$_2$(ox)(NO$_3$)$_6$(H$_2$O)$_2$]·1.2(H$_2$O)}$_n$ (**5**), {[Cu(dpp)(NO$_3$)](NO$_3$)·(H$_2$O)}$_n$ (**6**) and {[Cu(dpp)(SO$_4$)(H$_2$O)$_2$]}$_n$ (**7**), where acac$^-$ = acetylacetonate, ox^{2-} = oxalate. Remarkably, the treatment of Cu(II) chloride dihydrate with dpp in methanol solution led to an unusual *in situ* condensation of dpp with acac$^-$ to produce [Cu$_2$(acdpp)$_2$(Cl)$_4$]·2(MeOH) (**8**). The structure of **1** consists of neutral, mononuclear [Cu(acac)(dpp)(NO$_3$)] units with acac$^-$ and dpp acting as bidentate ligands. In **2**, the dpp ligand coordinates in a bis-chelating mode to two Cu(II) ions and bridges them in a dimeric entity, whereas an oxalate linker joins [Cu(Hdpp)(Cl)$_2$(H$_2$O)]$^+$ units into a dimer in **4**. The compounds **3**, **5**, **6** and **7** are 1D chain coordination polymers, which incorporate two symmetry independent metal centers and different bridging ligands: Hdpp$^+$ as a protonated cationic or dpp as a neutral chelating ligand and oxalate, Cl$^-$ anions or sulfate di-anions as bridging ligands. Magnetic studies were performed on samples **1** and **2**, and the analysis reveals a very weak magnetic exchange coupling mediated through the dpp ligand.

1 Introduction

The design and development of rational synthetic routes to metal-organic materials (MOMs) with target properties remains to be a challenge in materials science. Detailed understanding of different interactions involved in self-assembly processes [1-5] is essential for the development of such materials. The type and topology of the product generated from the self-assembly of metallo-organic species can be fine-tuned through judicious choice of both metal centers and organic ligands [6]. Along this line, interest has focused on transition metal complexes and coordination polymers using oxalate and/or N-donor chelating and bridging ligand systems, which may have applications as molecule based magnetic or chromophoric materials [7-11]. The 2,3-bis(2-pyridyl)pyrazine (dpp) ligand is a multifunctional ligand that shows several bonding modes and has been widely used in the design of numerous complexes with interesting properties. A detailed analysis of coordination modes of the dpp ligand in transition metal complexes, extracted from the Cambridge Structural Database (ConQuest Version 1.19, CSD version 5.38) [12], shows that dpp may adopt six different coordination modes leading to the formation of mononuclear as well as di- and polynuclear complexes. All coordination types of

2

the dpp ligand are shown in Scheme 1. The terminal five-membered chelate (**I**) (38 hits) [8,13-37] as well as bridging bis-bidentate chelate (**II**) (25 hits) [21,31,38-48] are the dominant ones for the dpp coordination. The terminal seven-membered bidentate mode (**III**) (9 hits) [49-54], the bidentate/monodentate mode (**IV**) (14 hits) [29,55-61], the bidentate/bis-monodentate mode (**V**) (1 hit) [55], and the bismonodentate mode (**VI**) (6 hits) [60-64] are less-common. In copper(II) complexes, most frequently the dpp ligand displays the coordination mode **I** (15 hits) [8,13,22,24,29,30,35,38,55], whereas the **II**, **IV**, and **V** coordination modes are quite rare: 8 hits for mode **II** [39,42-44], 3 hits for mode **IV** [29,55] and 1 hit for mode **V** [55]. Cu(II) compounds where the dpp ligand would possess coordination modes **III** and **VI** have not been found.
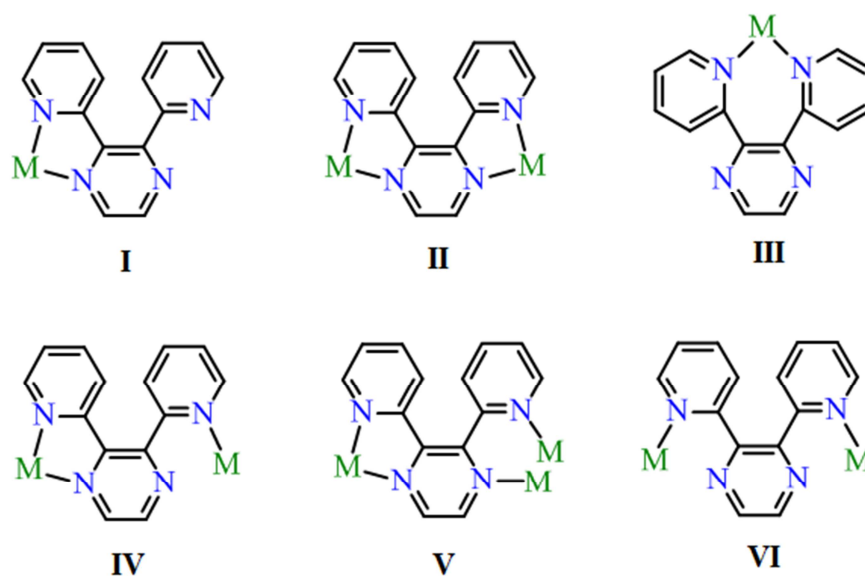
Scheme 1: Different coordination modes observed for the dpp ligand in metal complexes.

Principally, a diversity of structural motifs, including chain and framework structures are possible, making the dpp ligand an attractive choice in attempts to prepare porous compounds based on the assembly of organic molecules and metal-ion building blocks. Such supramolecular systems have gained considerable attention in recent times, especially due to their potential as functional materials with desired structures and properties. The bridging dpp ligand may be expected to propagate magnetic exchange between paramagnetic metal centers, and hence these compounds are also of interest for the study of magneto-structural relationships.

Continuing our studies of Cu(II) complexes with aromatic ligands [65-67], we report here the design and synthesis of a new series of Cu(II) complexes with the dpp ligand (Scheme 2), ranging from mononuclear $[Cu(acac)(dpp)(NO_3)]$ (**1**) and dinuclear $[Cu_2(acac)_2(dpp)(NO_3)(H_2O)]NO_3$ (**2**) and $[Cu_2(Hdpp)_2(ox)(Cl)_2(H_2O)_2]Cl_2 \cdot 6(H_2O)$ (**4**) compounds up to one-dimensional coordination polymers $\{[Cu_4(dpp)_2(ox)(Cl)_6]\}_n$ (**3**), $\{[Cu_4(dpp)_2(ox)(NO_3)_6(H_2O)_2] \cdot 1.2(H_2O)\}_n$ (**5**), $\{[Cu(dpp)(NO_3)](NO_3) \cdot (H_2O)\}_n$ (**6**) and $\{[Cu(dpp)(SO_4)(H_2O)_2]\}_n$ (**7**). Moreover, an unusual conversion of the dpp ligand in the presence of Cu(II) ions leading to the formation of a $[Cu_2(acdpp)_2(Cl)_4] \cdot 2(MeOH)$ (**8**) cluster has also been revealed. The thermal and magnetic properties of selected compounds have also been investigated.

4
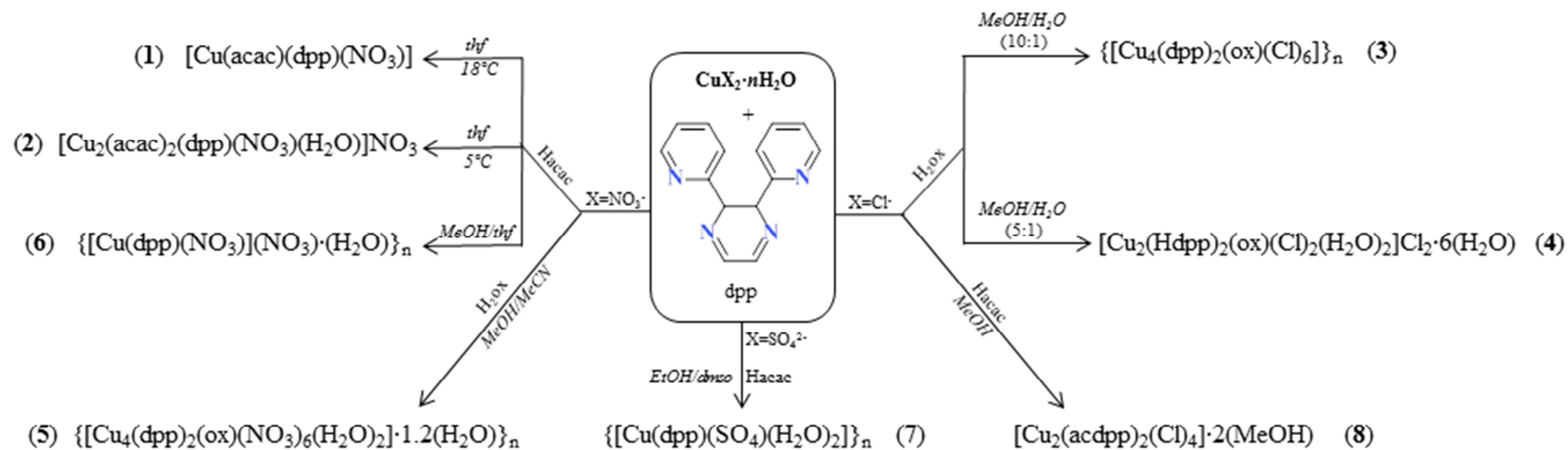
Scheme 2: Synthesis of Cu(II) complexes **1**-**8** with the dpp ligand.

2 Experimental section

2.1. Materials and methods

All reagents and solvents were obtained from commercial sources and were used without further purification. Infrared spectra were recorded on a FT IR Perkin-Elmer spectrometer using KBr pellets in the region 4000–650 cm^{-1}. TGA/DTA measurements were carried out with a Mettler Toledo TGA/SDTA 851 in dry N_2 (60 ml min^{-1}) at a heating rate of 10 K min^{-1}. Magnetic susceptibility data from powder samples were recorded using a Quantum Design MPMS-5XL SQUID magnetometer as a function of field (0.1 to 5.0 Tesla) and temperature (2.0 to 290 K). Experimental data were corrected for sample holder (PTFE capsules) and intrinsic diamagnetic contributions ($\chi_{m,dia}$ / 10^{-4} cm^3 K mol^{-1} = 2.29 (**1**), 3.51 (**2**)).

2.2. Syntheses

Synthesis of [Cu(acac)(dpp)(NO₃)] (1). To a solution of copper(II) nitrate trihydrate (0.024 g, 0.1 mmol) and 2,3-bis(2-pyridyl)pyrazine (0.023 g, 0.1 mmol) in 5 mL tetrahydrofuran, 0.01 mL acetylacetone was added. The resulting dark-green solution was filtered and the filtrate was stored at 18 °C in a closed vial for crystallization. Dark-green crystals of **1** suitable for X-ray measurements were filtered off after one week, washed with thf and dried in air. Yield: 0.0228 g, 50% based on copper. The complex **1** is soluble in MeOH, MeCN and insoluble in thf and dmf. Elemental analysis, found (calculated) for $C_{19}H_{17}CuN_5O_5$: C, 46.73 (49.73); H, 3.73 (3.73); N, 13.96 (15.26) %. IR data (KBr pellet, ν/cm^{-1}): 3423brw, 3086m, 2927sh, 2902sh, 2874sh, 1566vs, 1519vs, 1477m, 1383vs, 1310vs, 1298sh, 1230sh, 1170m, 1107w, 1070w, 1023m, 992m, 933m, 829w, 801sh, 786m, 760sh, 690w.

Synthesis of [Cu₂(acac)₂(dpp)(NO₃)(H₂O)]NO₃ (2). To a solution of copper(II) nitrate trihydrate (0.024 g, 0.1 mmol) and 2,3-bis(2-pyridyl)pyrazine (0.0117 g, 0.05 mmol) in 5 mL tetrahydrofuran, 0.01 mL acetylacetone was added. Slow evaporation of the filtrated dark-green solution at 5 °C gives dark-green crystals in four weeks. The crystals of **2** suitable for X-ray measurements were filtered off, washed with thf and dried in air. Yield: 0.016 g, 47% based on copper. The complex **2** is soluble in MeOH and dmf, and insoluble in thf and MeCN. Elemental analysis, found (calculated) for $C_{24}H_{26}Cu_2N_6O_{11}$: C, 41.63; 41.57 (41.07); H, 4.08; 3.63 (3.73); N, 12.03; 12.01 (11.98) %. IR data (KBr pellet, ν/cm^{-1}): 3431brw, 2958m, 2927sh, 2902sh,

6

2874sh, 1615vs, 1480m, 1459m, 1413s, 1370s, 1295m, 1230s, 1186m, 1054w, 1024s, 998vs, 893w, 867w, 816m, 803m, 777m, 709sh, 701m, 670m, 660sh.

Synthesis of {[Cu₄(dpp)₂(ox)(Cl)₆]}ₙ (3). To a solution of copper(II) chloride dihydrate (0.017 g, 0.1 mmol) and 2,3-bis(2-pyridyl)pyrazine (0.023 g, 0.1 mmol) in 5 mL MeOH, oxalic acid (0.009 g, 0.1 mmol) in 0.5 mL H_2O was added. The resulting green solution was filtered off and left for crystallization. The green crystals of **3** suitable for X-ray measurements were filtered off after one week, washed with MeCN and dried in air. Yield: 0.0035 g, 27% based on copper. The complex **3** is soluble in CH_2Cl_2, MeOH and H_2O and insoluble in thf. Elemental analysis, found (calculated) for $C_{15}H_{10}Cl_3Cu_2N_4O_2$: C, 35.32 (35.21); H, 2.47 (1.97); N, 9.92 (10.95) %. IR data (KBr pellet, v/cm^{-1}): 3440m, 3066w, 1642vs, 1471w, 1406m, 1363w, 1319w, 1294w, 1258w, 1236w, 1171sh, 1067w, 1023w, 876w, 819w, 792m, 771w, 751w, 666w.

Synthesis of [Cu₂(Hdpp)₂(ox)(Cl)₂(H₂O)₂]Cl₂·6(H₂O) (4). To a solution of copper(II) chloride dihydrate (0.017 g, 0.1 mmol) and 2,3-bis(2-pyridyl)pyrazine (0.023 g, 0.1 mmol) in 5 mL MeOH, oxalic acid (0.009 g, 0.1 mmol) in 1 mL H_2O was added. The resulting green solution was filtered off and left for crystallization. The green crystals of **4** suitable for X-ray measurements were filtered off after one week, washed with acetonitrile and dried in air. Yield: 0.035 g, 36% based on copper. The complex **4** is soluble in CH_2Cl_2, MeOH and H_2O, and insoluble in MeCN and thf. Elemental analysis, found (calculated) for $C_{30}H_{38}Cl_4Cu_2N_8O_{12}$: C, 46.22 (45.82); H, 4.91 (4.46); N, 14.38 (13.92) %. IR data (KBr pellet, v/cm^{-1}): 3390 brw, 3065brw, 1637vs, 1599sh, 1536m, 1472m, 1461m, 1405s, 1348m, 1306m, 1292m, 1260sh, 1240m, 1173sh, 1163m, 1153sh, 1111sh, 1061m, 1034s, 1023m, 930vw, 876m, 810sh, 789s, 771s, 747m, 666w.

Synthesis of {[Cu₄(dpp)₂(ox)(NO₃)₆(H₂O)₂]·1.2(H₂O)}ₙ (5). A green solution of copper(II) nitrate trihydrate (0.024 g, 0.1 mmol), 2,3-bis(2-pyridyl)pyrazine (0.0117 g, 0.05 mmol) and oxalic acid (0.009 g, 0.1 mmol) in MeCN/MeOH (1:1, 6 mL) was ultrasonicated for 40 min at 30 °C and then filtered. The filtrate was allowed to slowly evaporate at room temperature. After one week, plate green crystals of **5** suitable for X-ray measurements were filtered off, washed with MeOH and dried in air. Yield: 0.0042 g, 26% based on copper. Elemental analysis, found (calculated) for $C_{15}H_{14}Cu_2N_7O_{13.25}$: C, 28.71 (28.28); H, 2.25 (2.65); N, 15.63 (15.18) %. IR data (KBr pellet, v/cm^{-1}): 3750vw, 3443w, 3274vw, 3080w, 2926w, 2854vw, 1644m, 1603m,

1572vw, 1474vw, 1462w, 1417m, 1381w, 1305vw, 1278w, 1176vw, 1165w, 1137vw, 1116vw, 1065m, 1014vs, 911vw, 865w, 831vw, 814w, 788s, 743m, 709vw.

Synthesis of {[Cu(dpp)(NO$_3$)](NO$_3$)·(H$_2$O)}$_n$ (6). A green solution of copper(II) nitrate trihydrate (0.024 g, 0.1 mmol), 2,3-bis(2-pyridyl)pyrazine (0.0117 g, 0.05 mmol) and 0.01 mL acetylacetone in MeOH/thf (1:1, 6 mL) was ultrasonicated for 40 min at 30 °C and then filtered. The filtrate was allowed to slowly evaporate at room temperature. The green-blue crystals of **6** suitable for X-ray measurements were filtered off after one week, washed with MeOH and dried in air. Yield: 0.02 g, 45% based on copper. Elemental analysis, found (calculated) for C$_{14}$H$_{12}$CuN$_6$O$_7$: C, 38.23 (37.73); H, 2.75 (2.34); N, 19.11 (18.71) %. IR data (KBr pellet, ν/cm^{-1}): 3430w, 3081w, 1659m, 1603m, 1571vw, 1461s, 1416m, 1379w, 1342vw, 1303vw, 1294vw, 1277m, 1165s, 1136vw, 1116vw, 1065m, 1019s, 974vw, 918vw, 908vw, 869vw, 812m, 785m, 768w, 743w, 691vw, 665vw.

Synthesis of {[Cu(dpp)(SO$_4$)(H$_2$O)$_2$]}$_n$ (7). To a solution of copper(II) sulfate pentahydrate (0.025 g, 0.1 mmol) and dpp (0.023 g, 0.1 mmol) in 6 mL of a EtOH/dimethyl sulfoxide (1:1) mixture, 0.01 mL acetylacetone was added. The resulting green solution was filtered and this filtrate was kept at room temperature. The khaki crystals of **7** suitable for X-ray measurements were filtered off after six months, washed with EtOH and dried in air. Yield: 0.030 g, 70% based on copper. Elemental analysis, found (calculated) for C$_{14}$H$_{14}$CuN$_4$O$_6$S: C, 42.26 (41.83); H, 3.55 (2.95); N, 14.09 (13.64) %. IR data (KBr pellet, ν/cm^{-1}): 3833w, 3284vw, 3117vw, 3057w, 3004vw, 1671m, 1608m, 1583vw, 1557vw, 1483vw, 1472vw, 1438m, 1422m, 1400s, 1316vw, 1299m, 1247vw, 1215vs, 1182m, 1161w, 1143vw, 1124vw, 1101vw, 1095vw, 1061w, 1039vw, 1003vs, 951s, 872vw, 820w, 787s, 770w, 753m, 705w.

Synthesis of [Cu$_2$(acdpp)$_2$(Cl)$_4$]·2(MeOH) (8). To a solution of copper(II) chloride dihydrate (0.017 g, 0.1 mmol) and dpp (0.023 g, 0.1 mmol) in 5 mL MeOH, 0.01 ml acetylacetone was added. The resulting dark-green solution was filtered off and kept in a closed vial at room temperature. Slow evaporation during about eight months of this solution yielded brown prismatic single crystals of **8** for X-ray diffraction measurements. Yield: 0.008 g, 16% based on copper. Elemental analysis, found (calculated) for C$_{42}$H$_{36}$Cl$_4$Cu$_2$N$_8$O$_4$: C, 54.73 (54.32); H, 3.94 (3.54); N, 12.16 (11.76) %. IR data (KBr pellet, ν/cm^{-1}): 3502vw, 3070vw, 2924w, 1680vw, 1626vw, 1597w, 1586vw, 1566m, 1502m, 1480vw, 1459vw, 1449vw, 1409w, 1389s, 1361vw,

1352vw, 1288s, 1267w, 1237m, 1197w, 1165m, 1143vw, 1105vw, 1068m, 1016m, 1003vw, 988s, 938s, 901vw, 855w, 829m, 798vw, 774s, 758m, 746m, 717vw, 673s.

2.3. X-ray crystallography

X-Ray data were collected at room temperature on an Oxford Diffraction Xcalibur diffractometer equipped with a CCD area detector and a graphite monochromator utilizing MoK_a radiation (λ = 0.71073 Å). Final unit cell dimensions were obtained and refined on an entire dataset. All calculations to solve the structures and to refine the models proposed were carried out with the SHELX suite of programs [68]. In all structures, the C-bounded H-atoms were placed in calculated positions and were treated using a riding model approximation with $U_{iso}(H)$ = $1.5U_{eq}(C)$ for methyl group $1.2U_{eq}(C)$ for other hydrogen atoms, while the oxygen-bounded H-atoms were found from differential Fourier maps and refined isotopically with isotropic displacement parameter $U_{iso}(H)$ = $1.5U_{eq}(O)$. The X-ray data and the details of the refinement for **1 − 8** are summarized in Table 1, the selected geometric parameters are given in Table 1S. The figures were produced using the Mercury program [69].

Table 1

Crystal data and structure refinement for **1-8**.

Compound	1	2	3	4
Empirical formula	$C_{19}H_{17}CuN_5O_5$	$C_{24}H_{26}Cu_2N_6O_{11}$	$C_{15}H_{10}Cl_3Cu_2N_4O_2$	$C_{30}H_{38}Cl_4Cu_2N_8O_{12}$
Formula weight	458.92	701.59	511.70	971.56
T (K)	293(2)	293(2)	293(2)	293(2)
crystal system	monoclinic	monoclinic	triclinic	triclinic
space group	$P2_1/n$	$P2_1/c$	P-1	P-1
Z	4	4	2	1
a, Å	12.9681(5)	14.3459(6)	8.8654(7)	8.6798(10)
b, Å	10.6883(3)	12.1678(6)	10.4475(12)	10.294(3)
c, Å	13.9172(4)	15.9241(9)	10.6091(9)	12.243(4)
α (deg)	90	90	61.071(10)	69.64(2)
β (deg)	93.472(3)	95.003(5)	77.982(7)	72.54(2)
γ (deg)	90	90	83.395(8)	84.331(15)
V, Å^3	1925.46(12)	2769.1(2)	841.05(14)	978.3(4)
D_{calc} (g/cm^{-3})	1.583	1.683	2.021	1.649
μ(mm^{-1})	1.178	1.607	3.024	1.430
F(000)	940	1432	506	496

reflns collected/unique	6516 / 3577	10325 / 3359	4797 / 3115	5500 / 3412
rflns with $[I > 2\sigma(I)]$	2879	3359	2064	2533
data/restraints/parameters	3577 / 50 / 285	4898 / 25 / 414	3115 / 0 / 235	3412 / 12 / 256
goodness-of-fit on F^2	1.002	0.999	0.998	1.000
R_1, $wR_2[I > 2\sigma(I)]$	0.0414, 0.1078	0.0511, 0. 0.1144	0.0589, 0.1028	0.0444, 0.0912
R_1, wR_2(all data)	0.0560, 0.1166	0.0807, 0.1281	0.1035, 0.1169	0.0674, 0.0991
$\Delta\rho_{max}$, $\Delta\rho_{min}$ (e·Å^{-3})	0.448, −0.456	0.6154, −0.455	0.716, −0.709	0.363, −0.533

Compound	5	6	7	8
Empirical formula	$C_{15}H_{14}Cu_2N_7O_{13.25}$	$C_{14}H_{12}CuN_6O_7$	$C_{14}H_{14}CuN_4O_6S$	$C_{42}H_{36}Cl_4Cu_2N_8O_4$
Formula weight	631.41	439.84	429.89	985.67
Temperature (K)	293(2)	293(2)	293(2)	293(2)
Crystal system	triclinic	monoclinic	monoclinic	monoclinic
Space group	P-1	$P2_1/n$	$P2_1/c$	$C2/c$
Z	2	4	4	4
a, Å	8.5878(5)	12.7799(8)	14.4096(4)	23.4257(10)
b, Å	8.8927(4)	9.8365(7)	7.0000(2)	13.3795(5)
c, Å	14.5873(8)	14.3827(8)	21.0565(7)	13.9099(7)
α (deg)	75.489(4)	90	90	90
β (deg)	81.988(5)	111.017(7)	132.193(2)	111.862(5)
γ (deg)	89.460(4)	90	90	90
V, Å^3	1067.57(10)	1687.8(2)	1573.58(8)	4046.2(3)
D_{calc} (g/cm^{-3})	1.964	1.731	1.815	1.618
μ(mm^{-1})	2.081	1.349	1.565	1.371
$F(000)$	634	892	876	2008
reflns collect/unique	5778 / 3764	5662 /2968	6240 / 3506	6653 / 3748
rflns with $[I > 2\sigma(I)]$	3254	2448	2427	2499
data/restraints/params	3764 / 127/ 362	2968 / 3 / 259	3506 / 6 / 247	3748 / 0 / 276
goodness-of-fit on F^2	0.999	1.006	1.000	1.000
R_1, $wR_2[I > 2\sigma(I)]$	0.0357, 0.0954	0.0540, 0.1442	0.0553, 0.1036	0.0532, 0.1083
R_1, wR_2(all data)	0.0431, 0.1011	0.0676, 0.1536	0.0884, 0.1261	0.0920, 0.1224
$\Delta\rho_{max}$, $\Delta\rho_{min}$ (e·Å^{-3})	0.592, −0.462	1.559, −0.460	0.559, −0.522	0.475, −0.295

Table 2

Geometric parameters of hydrogen bonds (Å, deg) in **2**, **4**, **5**, **6**, **7** and **8**.

D–H⋯A	d(D–H)	d(H⋯A)	d(D⋯A)	∠(DHA)	Symmetry transformation for acceptor
2					
O1w–H1w1⋯O5	0.71(6)	2.12(6)	2.774(5)	153(8)	x, -y+1/2, z-1/2
O1w–H2w1⋯O8	0.87(6)	2.14(6)	2.987(9)	165(6)	x, -y+3/2, z+1/2
4					
O3w–H1w3⋯O2w	0.87	1.89	2.754(5)	171.1	-x+1, -y, -z+1
O3w–H2w3⋯Cl2	0.86	2.45	3.236(4)	152.9	-x+1, -y+1, -z
O2w–H2w2⋯Cl1	0.88	2.35	3.214(4)	167.8	x, y, z
O2w–H1w⋯O4w	0.88	1.91	2.768(4)	163.5	-x, -y+1, -z+1
O1w–H1w1⋯Cl2	0.87	2.48	3.236(3)	145.2	x+1, y, z
O1w–H2w1⋯O3w	0.87	1.96	2.820(4)	171.3	x, y, z
O4w–H2w4⋯Cl2	0.86	2.39	3.217(4)	162.8	x, y, z
N4–H1N⋯Cl2	0.86(4)	2.22(4)	3.054(3)	162(3)	x, y, z
5					
O1w–H1w1⋯O2w	0.87(2)	1.76(2)	2.627(5)	173(4)	x, y, z
O1w–H2w1⋯O1	0.87(2)	1.94(2)	2.796(3)	167(4)	-x, -y, -z+1
O2w–H1w2⋯O4	0.87(2)	2.32(5)	3.09(3)	148(7)	-x, -y, -z+1
O2w–H1w2⋯O5	0.87(2)	2.28(4)	3.085(11)	156(7)	-x, -y, -z+1
6					
O1w–H1w1⋯O4	0.87(2)	2.27(6)	3.003(8)	142(8)	-x, -y+1, -z
O1w–H2w1⋯O5	0.86(2)	2.08(5)	2.889(9)	157(10)	x, y, z
7					
O1w–H1w1⋯O1	0.85(2)	1.98(2)	2.822(4)	170(4)	-x+1, y-1/2, -z+1/2
O1w–H2w1⋯O4	0.85(2)	1.82(2)	2.637(4)	161(4)	-x+1, y+1/2, -z+1/2
O2w–H1w2⋯O2	0.85(2)	2.13(3)	2.954(5)	163(5)	-x+1, y-1/2, -z+1/2
O1w–H2w2⋯S1	0.85(2)	2.77(3)	3.424(3)	134(3)	-x+1, y+1/2, -z+1/2
O2w–H2w1⋯S1	0.85(2)	2.90(3)	3.677(4)	152(5)	-x+1, y-1/2, -z+1/2
O2w–H2w2⋯O4	0.88(2)	1.91(2)	2.779(5)	172(5)	x, y, z
O2w–H2w2⋯S1	0.88(2)	2.80(4)	3.565(4)	147(5)	x, y, z
8					
O1M–H1M⋯Cl1	0.82	2.69	3.367(6)	141.3	-x+3/2, -y+1/2, -z+1

3 Results and discussion

3.1 Synthesis and preliminary characterization

The variation in the storage temperature of the reaction mixture containing copper(II) nitrate trihydrate, 2,3-bis(2-pyridyl)pyrazine (dpp) and acetylacetonate (acac⁻) in tetrahydrofuran led to the mononuclear [Cu(acac)(dpp)(NO$_3$)] (**1**) compound formed at room temperature (18 °C), or the dinuclear [Cu$_2$(acac)$_2$(dpp)(NO$_3$)(H$_2$O)](NO$_3$) (**2**) compound which precipitated at lower temperature (5 °C) with a good yield of 50% and 47%, respectively (Scheme 2). The treatment of copper(II) chloride dihydrate salt with dpp and oxalic acid (H$_2$ox) in MeOH gave the 1D

11

coordination polymer $\{[Cu_4(dpp)_2(ox)(Cl)_6]\}_n$ (**3**) with 27% yield, however a small excess of water (1 mL compared to 0.5 mL) in the same reaction mixture led to the formation of the dimer $[Cu_2(Hdpp)_2(ox)(Cl)_2(H_2O)_2]Cl_2·6(H_2O)$ (**4**) in 36% yield. Ultrasonic treatment of the MeCN/MeOH mixture containing copper(II) nitrate trihydrate, dpp and oxalic acid led within one week to the precipitation of the 1D coordination polymer $\{[Cu_4(dpp)_2(ox)(NO_3)_6(H_2O)_2]·1.2(H_2O)\}_n$ (**5**), whereas the ultrasonic irradiation of copper(II) nitrate trihydrate, dpp, oxalic acid and acac⁻ in a MeOH/thf solution resulted in the 1D coordination polymer $\{[Cu(dpp)(NO_3)](NO_3)·(H_2O)\}_n$ (**6**). The reaction of copper(II) sulfate pentahydrate salt with dpp and acac⁻ in a 1:1 mixture of dimethyl sulfoxide and ethanol resulted in the 1D coordination polymer $\{[Cu(dpp)(SO_4)(H_2O)_2]\}_n$ (**7**). The identities of all compounds were determined by single crystal X-ray crystallography, and the homogeneity of samples was confirmed by elemental analysis and IR spectra.

The IR spectrum of a free dpp ligand was compared with the spectra of its Cu(II) complexes **1-7**. The characteristic absorption of the C=N groups of the aromatic rings which appears at 1655 cm⁻¹ in the spectrum of free dpp was observed to be shifted to 1658 cm⁻¹ (**6**) and 1671 cm⁻¹ (**7**) or overlaps with intense bands ν_{as}(C=C) + ν_{as}(C=O) of chelating acetylacetonate at 1566 cm⁻¹ (**1**), and ν_{as}(COO) of coordinated carboxylate groups of ox^{2-} ligands at 1642 (**3**), 1637 (**4**) and 1644 cm⁻¹ (**5**). The asymmetric and symmetric dpp aromatic ring stretching vibrations in the free ligand (1584, 1563, 1481, 1432 cm⁻¹) appear at 1603, 1571 and 1417 cm⁻¹ in coordination polymer **5**, at 1603, 1571 and 1416 cm⁻¹ in coordination polymer **6**, and at 1607, 1583, 1556, 1482, 1438, 1422 cm⁻¹ in coordination polymer **7**. The strong bands at 1381 cm⁻¹ in **5**, 1379 cm⁻¹ in **6**, and 1400 cm⁻¹ in **7** have been assigned to ν(C−N) stretching modes of vibrations of pyridine rings. The stretching vibrations of the coordinated NO_3^- anions in **5** appear at 1463, 1305, 1278, and 1014 cm⁻¹, and in **6** at 1461, 1303, 1277, and 1018 cm⁻¹ as strong-intensity bands, whereas the uncoordinated NO_3^- anion in **6** shows up as a shoulder at 1342 cm⁻¹. The strong bands at 1215, 1101, 1002 and 950 cm⁻¹ in **7** are ascribed to the coordinated SO_4^{2-} anion vibrations.

The presence of solvate and coordinated H_2O molecules in **4**, **5**, **6**, and **7** caused the appearance of broad bands in the range of 3442–3430 and 3383–3274 cm⁻¹, respectively, which were assigned to a ν(O−H) stretching vibration. In the case of **8**, a broad band at 3501 cm⁻¹ can be

attributed to the stretching vibration of solvate MeOH. In the range of 3117–2854 cm^{-1}, the asymmetric and symmetric C−H stretching vibrations for the aromatic rings of dpp and −CH$_3$ groups of acac$^-$ are observed.

Thermogravimetric analyses for **1**, **2** and **3** were performed in a nitrogen atmosphere in the temperature range of 25–800 °C. The mononuclear complex **1** is stable up to 150 °C and then the decomposition of the acetylacetonate ligand and nitrate anion takes place before 330 °C in two weakly resolved steps with a total weight loss of 30.9% (calculated 35.3%), accompanied by two observed exothermic process at 209 and 230 °C. For the dinuclear complex **2**, the exothermic removal of the organic part (two acetylacetonate and dpp ligands) and one coordinated water molecule with a weight loss of 59.4% (calculated 61.9%) is completed before 190 °C in one step, followed by the decomposition of the remaining nitrate anions. On further heating, the remaining dpp ligand decomposes. The TGA curve of **3** displays three main stages of weight losses. The weight loss from 60 to 225 °C of 15.8% corresponds to the loss of the oxalate anions (calculated 17.6%). The second weight loss stage occurs from 225 to 460 °C, where the curve shows the loss of 40.51% (calculated 45.8%) of two dpp molecules. The final step of the decomposition occurs within the temperature range 460-650 °C corresponding to the decomposition of the complexes with the formation of the CuO as a final product.

3.2 Structural studies

Compound **1** crystallizes in the monoclinic space group $P2_1/n$ and consists of neutral, mononuclear [Cu(acac)(dpp)(NO$_3$)] complexes. The Cu(II) cation is five-coordinated with two oxygen atoms of an acac$^-$ and two nitrogen atoms of a dpp ligand. The N$_2$O$_3$ square-pyramidal surrounding is completed with an O atom of NO$_3^-$ in the axial position at a distance of 2.460(2) Å. The four other metal-ligand distances Cu−N(O) in the basal plane are within the range 1.904(2) - 1.995(2) Å. The donor atoms in the equatorial plane of copper deviate from a mean plane within 0.131 - 0.142 Å showing a tetrahedral distortion, while the copper atom is displaced only by 0.096 Å from this plane toward the apical O3 atom. The dpp ligand adopts a chelating N,N′-coordination mode with the coordinated pyrazine and one pyridine ring forming a dihedral angle of 13.8°, while the second pyridine ring forms a dihedral angle of 65.9° with the pyrazine moiety. The acac$^-$ serves as a O,O′-chelating ligand, Figure 1a. In the crystal packing, two

neighboring complexes form a centrosymmetric dimer due to weak intermolecular interactions of the metal atom and the second pyridine moiety of dpp [Cu⋯N4, 3.255(2) Å], as well as π-π stacking interactions between aromatic rings of dpp ligands. Note, the dihedral angle in the stacking between overlapping pyridine and pyrazine rings equals 13.8° and the deviation of the atoms of pyridine ring from the plane of the pyrazine moiety is in the range of 3.253 - 3.912 Å; the interplanar separation between mean planes of overlapping fragments equals 3.427 Å, and the centroid⋯centroid distance is 3.851 Å, as shown in Figure 1b. The Cu1⋯Cu1* separation within the dimer is 7.617 Å.

(a)

(b)
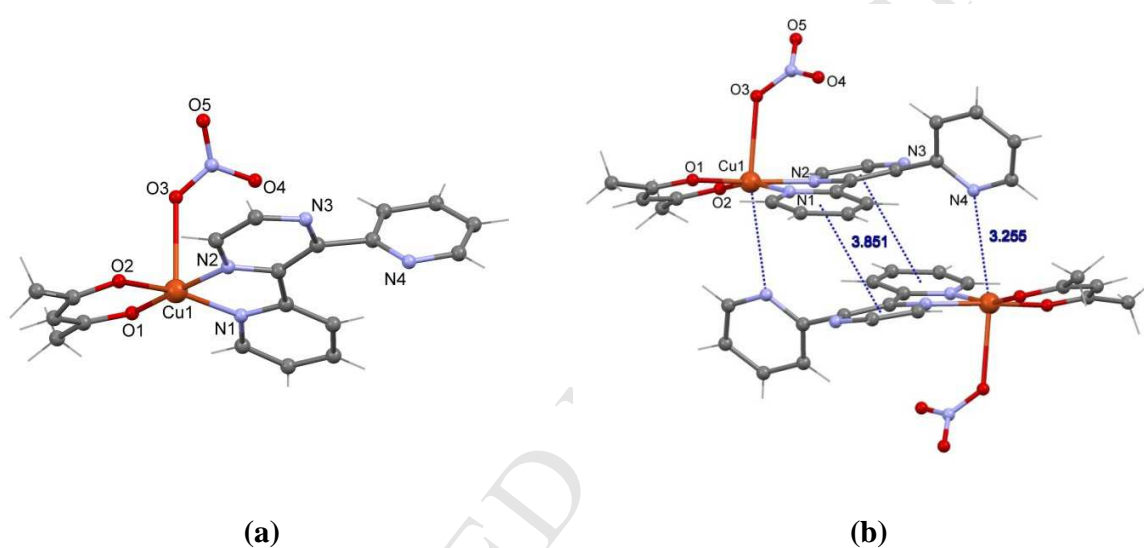
Figure 1 (a) View of the molecular structure of **1** with the partial atom numbering scheme, (b) The centrosymmetric dimer of **1**.

The binuclear compound **2** with the composition $[Cu_2(acac)_2(dpp)(NO_3)(H_2O)]NO_3$ contains two crystallographically independent Cu(II) atoms and crystallizes in the monoclinic space group $P2_1/c$. The bis-bidentate dpp ligand coordinates with all of its N atoms in a bis-chelating mode to two Cu(II) ions and bridges them in a dimeric entity, as shown in Figure 2a. The pyridyl rings of the dpp ligand form dihedral angles of 23.5 and 24.8° with pyrazine, and 46.6° with each other. The coordination of Cu(II) atoms adopts a distorted square pyramidal N_2O_3 geometry in which two N atoms of chelating dpp and two O atoms of chelating acac⁻ form the equatorial plane. The Cu–O distances in the basal plane fit in the narrow interval of 1.892(3) – 1.899(3) Å and the Cu–N distances are 1.970(3) – 2.026(3) Å. The Cu(II) deviations from basal planes toward the

axial ligands are equal to 0.071 Å for Cu1 and 0.104 Å for Cu2 atoms. The apical position in the vertex of the pyramid is occupied by a NO_3^- anion (Cu1) or a water molecule (Cu2) at distances Cu1–O3 = 2.352(3) Å and Cu2–O1w = 2.353(4) Å. An inter-sphere NO_3^- anion compensates the positive charge of the dinuclear complex. The packing in the crystal demonstrates the stacking interactions between the chelate ring formed by acac$^-$ ligand and fused chelate ring and pyrazine moiety of the dpp ligand from centro-symmetry related copper atoms [5], Figure 2b. The mutual arrangements of fragments involved in such interactions are similar for both copper atoms and characterized by next geometrical parameters: interplanar separations of overlapping fragments equal 3.377 and 3.509 Å, centroid···centroid distances between acac$^-$···dpp chelate rings are 3.707 and 3.973 Å and between acac$^-$ chelate ring···pyrazine moiety are 3.742 and 4.018 Å, and Cu···Cu separations are 3.762(7) and 4.094(9) Å for Cu1 and Cu2 atoms, respectively Figure 2c. These stacking interactions unite binuclear complexes **2** in well-defined chains along the crystallographic a axis. The chains are interconnected in the crystal by O1w–H···O5 = 2.774(5) Å hydrogen bonds between coordinated NO_3^- anions and water molecules. The disordered outer sphere NO_3^- anions are weakly H-bonded with the coordinated water molecules [O1w–H···O8, 2.987(9) Å], Table 2.

(a)   **(b)**

(c)
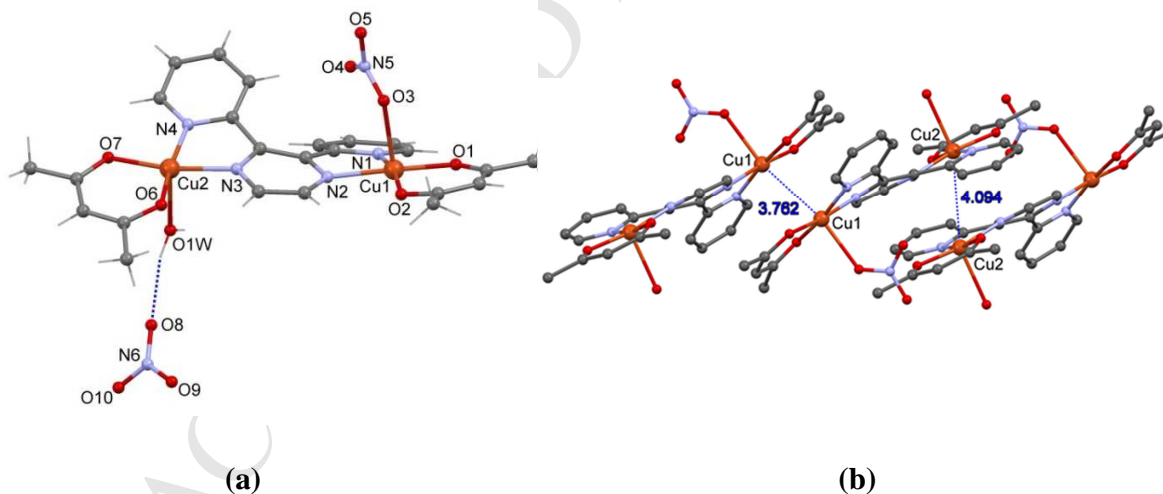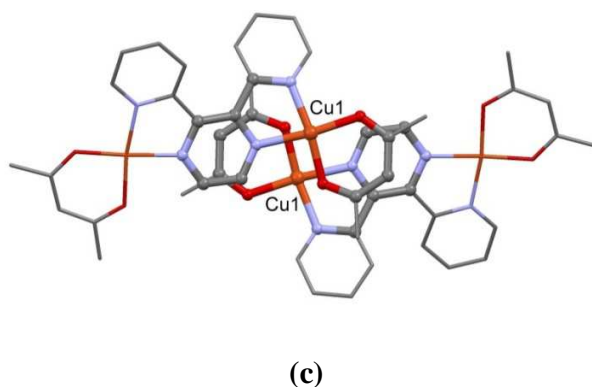
Figure 2 (a) View of the crystal structure of **2** with the partial atom numbering scheme, (b) Stacking-like interactions in **2**, (c) The manner of overlapping of stacked fragments (highlighted).

Compound **3**, $\{[Cu_4(dpp)_2(ox)Cl_6]\}_n$, crystallizes in the triclinic centrosymmetric space group *P*-1 and represents a 1D coordination polymer with three different bridging ligands: dpp, oxalate and Cl⁻ anions. The dpp ligand chelates two symmetry independent metal ions to form a binuclear unit. The pyridyl rings of the dpp ligand form dihedral angles of 20.6° and 36.6°, respectively with the pyrazine plane and 57.05° with each other. The oxalate bridge from one side and two Cl⁻ anions from other site connect the neighboring centro-symmetry related binuclear units in 1D chains, as shown in Figure 3. The square-pyramidal N_2O_2Cl surrounding of Cu1 atom is completed by two O atoms from the oxalate bridging ligand, two N atoms of the chelating dpp ligand [Cu1–N(O), 1.986(5) – 2.016(5) Å] and a terminal chlorine in the apex of the pyramid at the 2.401(2) Å. The square-pyramidal N_2Cl_3 coordination of Cu2 atom is accomplished by two N atoms of the chelating dpp ligand [Cu2–N distances equal 1.998(5) and 2.113(5) Å], terminal Cl2 [Cu2–Cl2, 2.217(2) Å] and bridging Cl3 [Cu–Cl3, 2.254(2) Å] in the basal plane, and centro-symmetry related Cl3* in the vertex of the pyramid [Cu2–Cl3*, 2.597(2) Å], Figure 3. Thus, centrosymmetric oxalate dianion bridges two symmetry related Cu1 atoms, while two mono *µ*-chloro ligands bridge the inversion center related Cu2 atoms. There are three different intrachain Cu⋯Cu separations, namely 6.719(1) Å through the dpp ligand, 5.173(1) Å for Cu1-ox-Cu1, and the shortest one 3.252(1) Å through the double chlorine bridge. The Cu2-Cl3-Cu2 bridging angle is 83.9º. In the crystal, parallel chains run along the [102] direction. The crystal packing does not reveal any pronounced specific interchain interactions.
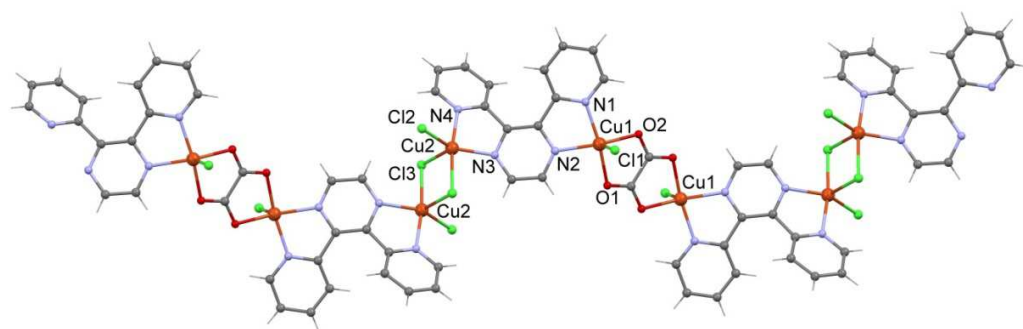
Figure 3 Fragment of the polymeric chain in the crystal structure of **3** with the partial atom numbering scheme.

Compound **4**, $[Cu_2(Hdpp)_2(ox)(Cl)_2(H_2O)_2]Cl_2 \cdot 6(H_2O)$, crystallizes in the triclinic centrosymmetric space group *P*-1 and comprises the cationic binuclear complex which resides on an inversion center. In contrast to compound **3**, where the copper atom adopts a square-pyramidal surrounding, the metal atoms adjust a 4+1+1 square-bipyramidal coordination with a N_2O_3Cl core in **4**. The coordination sphere of the Cu(II) atom in **4**, Figure 4a includes two N atoms of a chelating monoprotonated Hdpp$^+$ ligand [Cu1–N, 1.972(3) - 2.023(3) Å], two O atoms from an oxalate chelate-bridging ligand [Cu1–O, 1.975(2) - 2.014(2) Å] in the basal plane, and a chlorine anion and a weakly coordinated water molecule [Cu1–Cl1, 2.498(2) Å and Cu1–O1w, 2.757(4) Å] in the vertexes of the bipyramid. The pyridyl rings of the dpp ligand form dihedral angles of 21.98° and 42.75°, respectively with the pyrazine plane and 61.87° with each other. The oxalate bridges two Cu(II) atoms in a dimer with Cu···Cu separation of 5.174(1) Å. The crystal structure of **4** reveals the formation of an unusual cyclic eight-membered hybrid water-chloride $[(H_2O)_6(Cl)_2]^{2-}$ cluster, Figure 4b. The hydrogen-bonding patterns of clusters is described by a $R^6_8(16)$ graph set, Table 2. In the crystal packing, the cluster is H-bonded with eight surrounded cationic complexes, which completely encapsulate it, Figure 4c.

17

(a)

(b)

(c)
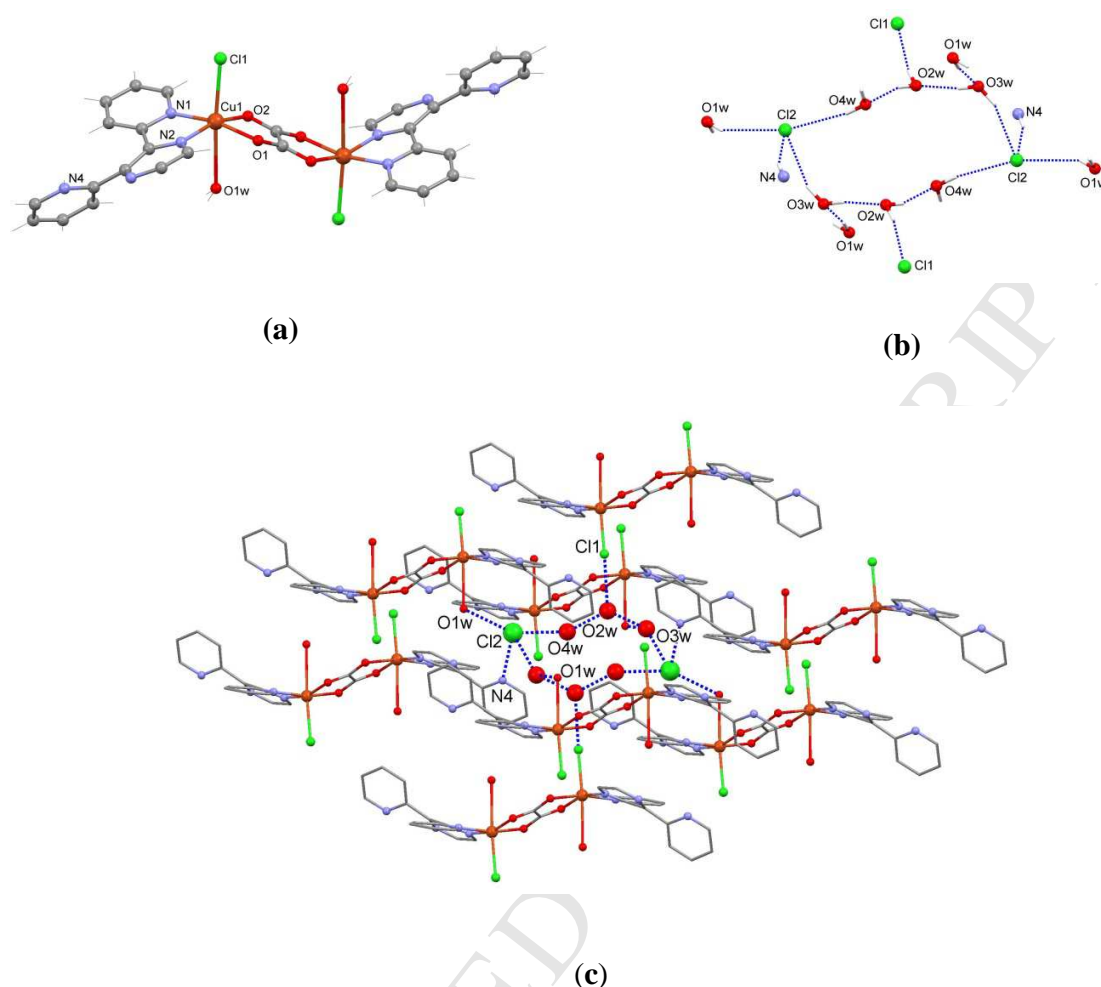
Figure 4 (a) View of the molecular structure of **4** with the partial atom numbering scheme, (b) Hybrid water-chloride cyclic $[(H_2O)_6(Cl)_2]^{2-}$ anionic cluster and surrounding H-bonded atoms of cationic binuclear complexes, (c) Fragment of packing illustrating the encapsulation of the hybrid cluster in the structure of **4**; the atoms of the cluster are shown by bigger diameter balls.

The anhydrous coordination polymer **3** and water rich compound **4** have been obtained by similar synthetic protocols and differ only by the amount of water in the reaction. Their comparison indicates the dramatic influence of water on the structure of final products. Thus, the promiscuity of water molecules demonstrates that composition and structure remain largely unpredictable, and water is indeed the nemesis of crystal engineering [70].

Compound **5**, $\{[Cu_4(dpp)_2(ox)(NO_3)_6(H_2O)_2]\cdot 1.2(H_2O)\}_n$, crystallizes in the triclinic centrosymmetric space group *P*-1 and contains the polymeric ribbons build-up from tetranuclear units. The neutral dpp ligand chelates two symmetry-independent Cu(II) atoms and an oxalate dianion joins these couples in a centrosymmetric tetranuclear unit through a bis-chelate function, Figure 5a. The pyridyl rings of the dpp ligand form dihedral angles of 25.1° and 27.4°, respectively with the pyrazine plane and 51.1° with each other. In the crystal, the tetranuclear units are extended into ribbons along the *a* axis due to a bridging function of one nitrate anion, which coordinates to Cu1 [Cu1–O4, 2.130(3) Å] and weakly coordinates to Cu2 atoms of the neighboring, related by translation *a,* tetranuclear unit [Cu–O5*, 2.680(1) Å], Figure 5b. The Cu⋯Cu separations in the ribbon are 5.100, 6.686, and 6.634 Å through oxalate, dpp and bridging NO_3^-, respectively. Additionally to dpp, the Cu1 atom coordinates a water molecule and two NO_3^- anions, and the N_2O_3 surrounding of the metal may be described as intermediate between a distorted square pyramidal and distorted trigonal-bipyramidal [Cu1–N, 2.004(3) – 2.014(3) Å and Cu1–O, 1.953(2) – 2.130(3) Å]. The degree of distortion is indicated by the general descriptor $\tau = (\beta - \alpha)/60$ for five-coordinated complexes [71–73], where α and β are two largest angles at the metal center. For the idealized square pyramid and trigonal bipyramid, extremes are $\tau = 0$ and 1, respectively, and τ equals 0.57 in complex **5** for the Cu1 atom. The N_2O_4 square-bipyramidal 4+1+1 coordination surrounding of the Cu2 atom is provided by two chelate ligands in the basal plane [Cu2–N, 1.956(3) and 2.003(3) Å; Cu2–O, 1.956(2) and 1.967(2) Å], and two NO_3^- anions in apical positions [Cu2–O, 2.333(3) and 2.679(3) Å].

The ribbons are H-bonded through coordinated and solvent water molecules into layers parallel to the *ac* plane, Table 2. The crystal packing points to stacking interactions between the centrosymmetry related pyridine moieties of dpp ligands of neighboring parallel layers with the interplanar separation of 3.463 and 3.367 Å and centroid⋯centroid distances of 3.748 and 4.081 Å.

a

b

Figure 5 (a) View of a tetramer with the partial atom numbering scheme and (b) fragment of ribbon in **5**.

Compound **6**, $\{[Cu(dpp)(NO_3)](NO_3)\cdot(H_2O)\}_n$, crystallizes in the monoclinic centrosymmetric space group $P2_1/n$ and consists of $[Cu(NO_3)]^+$ units joined by dpp into cationic zigzag chains, outer sphere NO_3^- anions and solvate water molecules [74]. The pyridyl rings of the dpp ligand form dihedral angles of 23.9° and 37.5°, respectively with the pyrazine plane and 58.2° with each other. In the structure of **6**, the cationic zigzag chains run along the crystallographic *b* axis as shown in Figure 6. The Cu(II) atoms adjust a N_4O square-pyramidal coordination environment accomplished by four N atoms of two bridging chelating dpp ligands and an O atom of the nitrate anion. The Cu−N(O) distances in the basal plane are within the range 1.975(3) - 2.059(3) Å, and the Cu1−N2 distance to the vertex of the pyramid equals 2.241(3) Å. The metal atom displaces from the mean plane of the base in the direction of the vertex of the pyramid by 0.129 Å. The Cu···Cu separation along the polymeric zigzag chain is 6.878 Å. The parallel packing of chains creates hydrophobic cavities filled by cyclic $[(H_2O)_2(NO_3)_2]^{2-}$ anionic clusters with a $R_4^4(12)$ graph set of H-bonds pattern, Table 2.

Figure 6 Packing of chains and encapsulation of anionic clusters in **6** with the partial atom numbering scheme.

Compound **7**, $\{[Cu(dpp)(SO_4)(H_2O)_2]\}_n$, crystallizes in the monoclinic centrosymmetric space group $P2_1/c$ and its structure consists of $[Cu(dpp)(H_2O)_2]^{2+}$ entities linked by bridging SO_4^{2-} anions into neutral 1D helix-like chains along the crystallographic *b* axis, Figure 7. The square-bipyramidal 4+1 coordination with N_2O_4 surrounding of the Cu(II) atom is completed in the basal plane by two N atoms of a chelate dpp ligand [Cu−N, 1.988(3) and 2.006(4) Å], a water molecule [Cu1−O1w, 1.965(3) Å] and oxygen of SO_4^{2-} dianion at the Cu1−O1 = 1.964(3) Å distance. Another water molecule [Cu1−O2w, 2.570(4) Å] and an oxygen atom [Cu1−O2, 2.371(3) Å] of SO_4^{2-} related by a two-fold screw axis occupy the apical positions. The Cu···Cu separation along the chain equals 5.1237(9) Å. The O−H···O hydrogen bonds additionally link monomeric units within the chains, Table 2. The infinite π–π stacking interactions between nearly parallel pyridine and pyrazine moieties of interdigitated adjacent chains unite them in supramolecular layers parallel to the crystallographic *ab* plane. The dihedral angle between pyridine and pyrazine moieties in the stack equals 3.07º, centroid···centroid separations are 3.568 and 3.928 Å, and deviations of the atoms of pyridine rings from the plane of the pyrazine moiety along the stack are in the ranges 3.308 - 3.449 and 3.219 - 3.360 Å, respectively.
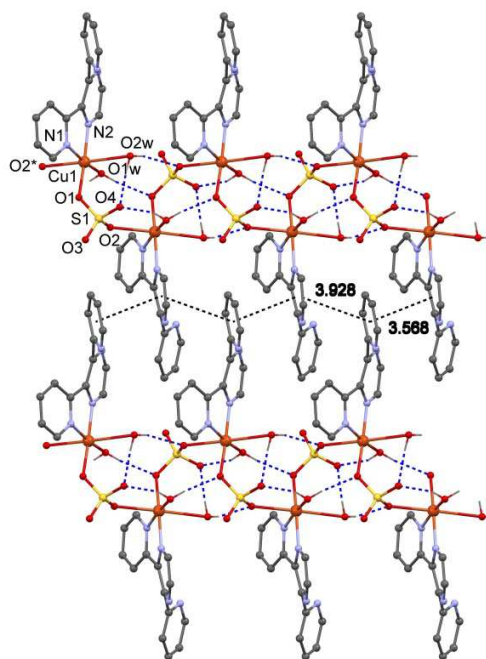
Figure 7 View of a fragment of polymeric chains and infinite stacking of neighboring chains in **7** with the partial atom numbering scheme.

Compound **8** with the composition [Cu$_2$(acdpp)$_2$Cl$_4$]·2(MeOH) crystallizes in the monoclinic space group *C*2/*c*. It reveals a dimeric dinuclear neutral complex, Figure 8 with unprecedented ligands obtained *in situ* as the product of dpp and Hacac condensation. The ligand comprises an aromatic C5 ring fused with a pyrazine moiety. The possible way of the condensation reaction is shown in Scheme 1S. The dimer resides on a two-fold axis, thus having C_2 molecular symmetry. The N$_3$OCl surrounding of the metal can be described as intermediate between a distorted square pyramidal and trigonal-bipyramidal; the τ descriptor equals 0.496. The tetradentate NNNO monoanionic acdpp$^-$ ligand coordinates to Cu1 atom in a NNO manner, forming coplanar five- and six-membered metallacycles [Cu−N1/N2 = 1.961(3)/2.014 Å, Cu1−O1 = 1.968(3) Å]. The N4 atom coordinates to the symmetry related metal atom in dimer [Cu1−N4, 2.270(3) Å]. The coordination environment of the Cu(II) atom is accomplished by a chlorine atom at the distance of 2.284(2) Å.

The Cu1 atom and atoms of the organic ligand, except one pyridine ring and H-atoms of methyl groups, are close to a common plane within -0.118-0.141 Å, and the dihedral angle between this plane and the non-coplanar pyridine ring equals 86.99º. The extended planar

fragments are nearly parallel in the dimer, forming a dihedral angle of only 0.15º and their rings, involving metallacycles, are completely overlapped indicating the stacking interactions, Figure 8b. The deviation of atoms of the rings from the mean plane of symmetry related rings system in the dimer ranges from 3.263 to 3.467 Å. The aromatic C5 rings overlap in a face-to-face manner with centroid···centroid separation of 3.429 Å and other rings overlap in an offset–stacked mode with centroid-centroid separations for pyrazine···pyrazine being 3.506 Å, for pyridine···pyridine - 3.590 Å, for pyrazine···six-membered metallacycle - 3.525 Å, for pyrazine···five-membered metallacycle - 3.734 Å, and five-membered···five-membered metallacycle - 3.659 Å. The crystal packing of **8** reveals a formation of the "bricks wall" layer motif parallel to the (011) crystallographic plane and is sustained by the π−π-stacking interactions between the binuclear complexes, Figure 8c. In this stacking assembly the parallel center-symmetry related pyridine moieties overlap with the interplanar distance and centroid−centroid separation being 3.458 and 3.578 Å, respectively, and the similar pattern of stacking takes place for the aromatic C5 rings with interplanar distance and centroid−centroid separation being 3.488 and 3.621 Å, respectively. These "bricks wall" like parallel layers further interact along the crystallographic *a* axis through π-π stacking of pyridine moieties, that do not participate in intradimer stacking, and the interplanar distance and centroid−centroid separation equal 3.492 and 3.619 Å, respectively Figure 8 c,d. The remarkable feature of structure **8** is that the stacking interactions are the main driving forces in the formation of both molecular and crystal structures.

a

b

(c)   (d)
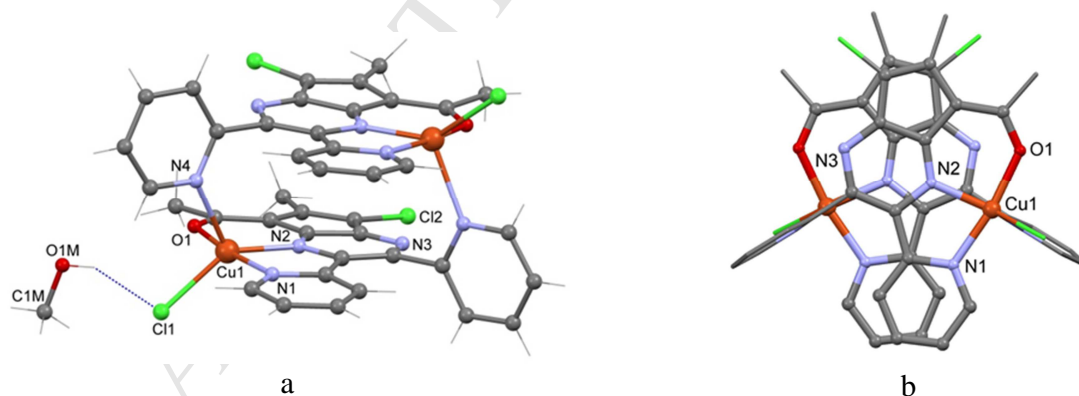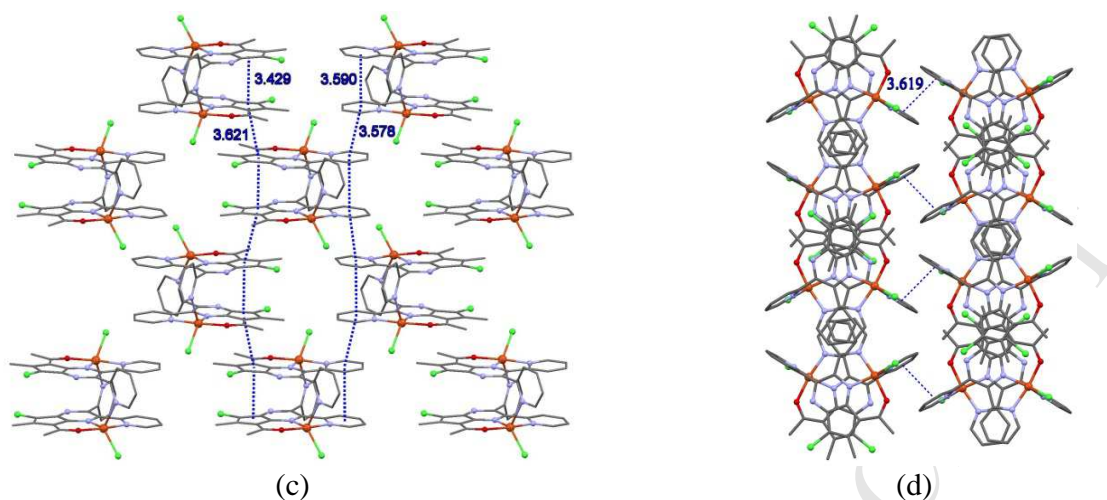
Figure 8 (a) Formula unit of **8** with the partial atom numbering scheme, (b) The manner of intra-dimer stacking in **8**; view perpendicular to the mean plane of the ring system; fragments participating in stacking interactions are highlighted, (c) The "bricks wall" infinite stacking motif in the structure **8**, (d) The inter-layer stacking interactions.

3.3 Magnetic properties

The temperature and field dependent magnetic measurements of **1** and **2** are represented by $\chi_m T$ vs. T and M_m vs. B plots in Figure 9. For **1**, the $\chi_m T$ value of 0.43 cm^3 K mol^{-1} at 290 K and 0.1 T lies within the expected[75] range 0.36 – 0.61 cm^3 K mol^{-1} for an isolated Cu(II) center. By cooling the compound, the value of $\chi_m T$ stays almost constant over the measured temperature range, slightly decreasing to 0.41 cm^3 K mol^{-1} at 2.0 K. The molar magnetization at this temperature is a linear function of the applied field up to approximately 1.5 T, and reaches 1.0 $N_A \mu_B$ at 5.0 T without being saturated. Both data are in agreement with a single isolated Cu(II) center, which is characterized by a distorted square-planar or square-pyramidal coordination sphere. For **2**, the respective $\chi_m T$ vs. T and M_m vs. B curves show similar shapes as for **1**. This is expected because **2** is approximately the dimer of **1** for which one NO$_3^-$ ligand is substituted by a comparable ligand, a water molecule, and the Cu(II) centers are almost isolated. At 290 K and 0.1 T, the $\chi_m T$ value is 0.86 cm^3 K mol^{-1} well within the expected[75] range 0.72 – 1.21 cm^3 K mol^{-1} for two non-interacting Cu(II) centers, Figure 9. By decreasing temperature, $\chi_m T$ linearly decreases to 0.83 cm^3 K mol^{-1} at 25.0 K, and subsequently drops to 0.68 cm^3 K mol$^-$

[1] at 2.0 K indicating weak antiferromagnetic exchange interactions. At 2.0 K, the molar magnetization continuously increases reaching 1.9 $N_A \mu_B$ at 5.0 T. Taking into account structural information, the exchange interactions are most likely mainly of intramolecular than of intermolecular nature due to the exchange pathway via the π-system of the dpp ligand although the intermolecular copper-copper distances are shorter.
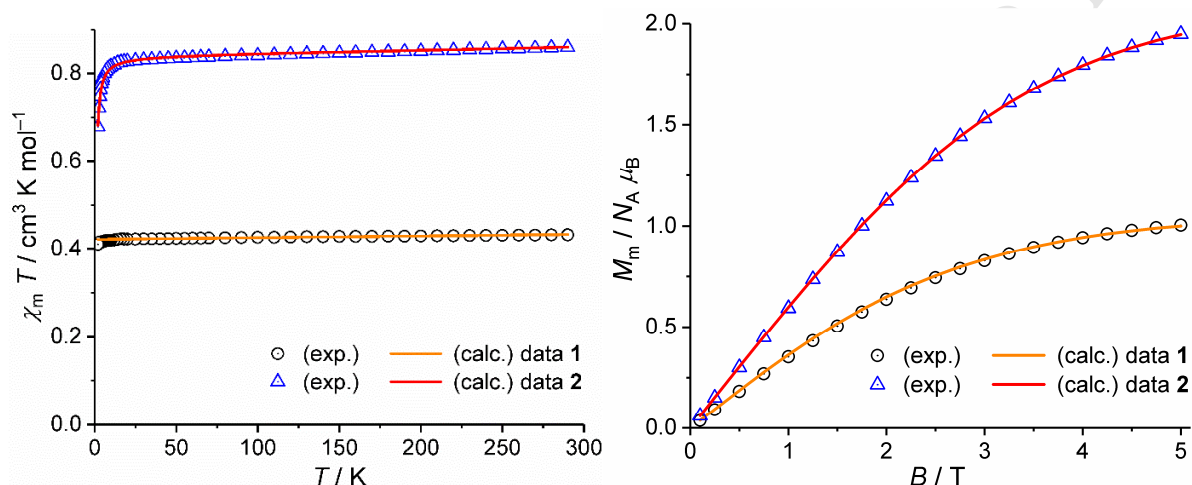
Figure 9 Temperature dependence of $\chi_m T$ at 0.1 T of **1** and **2** (left), and molar magnetization M_m vs. applied field B at 2.0 K (right).

To quantify the magnetic properties of **1** and **2**, the data were analyzed employing the computational framework CONDON 2.0 [76-78]. We consider spin-orbit coupling, electron-electron interrepulsion and Zeeman effect by adopting the corresponding parameters (one electron spin-orbit coupling constant ζ, Racah parameters B and C) from literature [78]. In addition, the ligand field is approximated assuming a ligand field symmetry of C_{4v} represented by the parameters B^2_0, B^4_0 and B^4_4 (Weybourne notation), which are varied in the fitting procedure. In case of **2**, both Cu(II) centers are treated to be identical, and exchange interactions are included using the Heisenberg Hamiltonian $-2J\, S_{Cu1} \cdot S_{Cu2}$. The results of the least-squares fits are given in Table 3. For **1**, the parameters represent an isolated Cu(II) ion in a ligand field of square-pyramidal geometry with elongated height, yielding a well isolated ground doublet. For **2**, the parameters are moderately different representing a slightly greater height of the square-pyramidal coordination sphere, which is potentially due to the approximation of two identical

Cu(II) centers. The exchange coupling parameter J describes very weak antiferromagnetic exchange interactions between both Cu(II) centers.

Table 3

Parameters of magnetochemical analysis of **1** and **2**.

	1	**2**
ζ / cm^{-1} [76]	829	
B / cm^{-1} [76]	1238	
C / cm^{-1} [76]	4659	
B^2_0 / cm^{-1}	-14002 ± 888	-26635 ± 731
B^4_0 / cm^{-1}	29202 ± 493	30461 ± 406
B^4_4 / cm^{-1}	33943 ± 4257	33276 ± 415
J / cm^{-1}	——	-0.46 ± 0.08
SQ	1.1 %	0.5 %

(SQ: relative root mean square error)

4 Conclusion

In summary, seven new copper(II) coordination compounds with 2,3-bis(2-pyridyl)pyrazine of different nuclearity and topology have been successfully synthesized by varying the starting copper salts, second organic ligand (Hacac or H_2ox), solvents or temperature. Our study demonstrates that only by simply changing of the crystallization temperature (**1** and **2**) or amount solvent water (**3** and **4**) under similar synthetic conditions results in rich structural chemistry and topologies. The ability to generate different coordination compounds (copper monomer, dimer, or polymer) *in situ*, by controlling the crystallization temperature or solvent system, presents a prospective route for the design of novel materials with different topologies and properties. Extraordinarily, the dimeric neutral complex **8,** [Cu$_2$(acdpp)$_2$(Cl)$_4$]·2(MeOH), with unprecedented anionic ligands was obtained *in situ* due to dpp and Hacac condensation. In this study we did not aim to give a full account on the magnetic properties of all compounds; this aspect would be beyond the scope of the paper. However, we focused on samples **1** and **2** in order to give an example for an exchange interaction through the neutral bridging dpp ligand, which turns out to be very weakly antiferromagnetic within the actual structure.

5 Supplementary data

Scheme of the formation of complex **8**, and table of selected bond lengths and angles in **1-8.**

CCDC 1824612-1824619 contain the supplementary crystallographic data for this paper. These data can be obtained free of charge via www.ccdc.cam.ac.uk/data_request/cif, or by emailing data_request@ccdc.cam.ac.uk, or by contacting The Cambridge Crystallographic Data Centre, 12 Union Road, Cambridge CB2 1EZ, UK; fax: +44 1223 336033.

AUTHOR INFORMATION

Corresponding Authors

*E-mail: kravtsov@phys.asm.md . Tel.: +373 22738154. Fax: 373 22 725887.

*E-mail: sbaca_md@yahoo.com

References

[1] H.W. Roesky, M. Andruh, Coord. Chem. Rev., 236 (2003) 91–119.

[2] A.M. Madalan, V.Ch. Kravtsov, D. Pajic, K. Zadro, Yu.A. Simonov, N. Stanica, L. Ouahab, J. Lipkowski and M. Andruh, Inorg. Chim. Acta, 357 (2004) 4151–4164.

[3] A.M. Madalan, N. Avarvari and M. Andruh, Crystal Growth & Design, 6 (2006) 1671-1675.

[4] A.M. Madalan, M. Andruh, N. Avarvari and M. Fourmigué, Metal-Organic, and Nano-Metal Chemistry, 37 (2007) 757–764.

[5] D.P. Malenov, G.V. Janjic´, V.B. Medakovic´, M.B. Hall and S.D. Zaric, Coord. Chem. Rev., 345 (2017) 318-341.

[6] A.B. Lysenko, G.A. Senchyk, L.V. Lukashuk, K.V. Domasevitch, M. Handke, J. Lincke, H. Krautscheid, E.B. Rusanov, K.W. Krämer, S. Decurtins and S.-X. Liu, Inorg. Chem., 55 (2016) 239-250.

[7] S. Decurtins, H.W. Schmalle, P. Schneuwly, L.-M. Zheng, J. Ensling, A. Hauser, Inorg. Chem., 34 (1995) 5501-5506.

[8] J. Carranza, H. Grove, J. Sletten, F. Lloret, M. Julve, P. E. Kruger, Ch. Eller and D.P. Rillema, Eur. J. Inorg. Chem., 24 (2004) 4836-4848.

[9] C. Goze, N. Dupont, E. Beitler, C. Leiggener, H. Jia, P. Monbaron, S.-X. Liu, A. Neels, A. Hauser and S. Decurtins, Inorg. Chem., 47 (2008) 11010-11017.

[10]   Y.-F. Ran, S.-X. Liu, O. Sereda, A. Neels and S. Decurtins, Dalton Trans., 40 (2011) 8193-8198.

[11]   S. Decurtins, R. Pellaux, A. Hauser and M.E. von Arx, In Magnetism: A Supramolecular Function, (Ed.: O. Kahn), Cluwer Academic Publisher, Dordrecht, NATO ASI Series C-484 (1996) 487-508.

[12]   C.R. Groom, I.J. Bruno, M.P. Lightfoot and S.C. Ward, Acta Crystallogr., B72 (2016) 171–179.

[13]   V. Tudor, T. Mocanu, F. Tuna, A.M. Madalan, C. Maxim, S. Shova and M. Andruh, J. Mol. Struct., 1046 (2013) 164-170.

[14]   A. Jain, C. Slebodnick, B.S.J. Winkel and K.J. Brewer, J. Inorg. Biochem., 102 (2008) 1854-1861.

[15]   K. Ha, Acta Crystallogr., Sect. E: Struct. Rep. Online 67 (2011) m1230.

[16]   K. Ha, Acta Crystallogr., Sect. E: Struct. Rep. Online 67 (2011) m1454.

[17]   Y.-Y. Choi and W.-T. Wong, J. Chem. Soc., Dalton Trans., 3 (1999) 331-338.

[18]   A. Grirrane, A. Pastor, E. Alvarez, C. Mealli, A. Ienco, P. Rosa and A. Galindo, Eur. J. Inorg. Chem., (2007) 3543-3552.

[19]   D. Armentano, G. de Munno, F. Guerra, J. Faus, F. Lloret and M. Julve, Dalton Trans., (2003) 4626-4634.

[20]   M.B. Ferrari, G.G. Fava, G. Pelosi, G. Predieri, C. Vignali, G. Denti and S. Serroni, Inorg. Chim. Acta, 275 (1998) 320-326.

[21]   F. S. Delgado, F. Lahoz, F. Lloret, M. Julve and C. Ruiz-Perez, Crystal Growth & Design, 8 (2008) 3219-3232.

[22]   J.R. Kirchhoff and K. Kirschbaum, Polyhedron, 17 (1998) 4033-4039.

[23]   K.T. Brooks, D.C. Finnen, , J.R. Kirchhoff and A.A. Pinkerton, Acta Crystallogr., Sect. C: Cryst. Struct. Commun. 50 (1994) 1696-1699.

[24]   S. Berger, T. Scheiring, J. Fiedler and W.Z. Kaim, Z. Anorg. Allg. Chem., 630 (2004) 2409-2417.

[25]   S.K. Singh, M. Chandra, S.K. Dubey and D.S. Pandey, Eur. J. Inorg. Chem., 19 (2006) 3954-3961.

[26]   R.A. Machado, M.C. Goite, A.J. Arce, Y. De Sanctis, A.J. Deeming, L. D'Ornelas and D.A. Oliveros, J. Organomet. Chem., 690 (2005) 622-628.

[27]   F. Kennedy, N.M. Shavaleev, T. Koullourou, Z.R. Bell, J.C. Jeffery, S. Faulkner and M.D. Ward, Dalton Trans., (2007) 1492-1499.

[28]   R.S. Rarig Junior, P.J. Hagrman and J. Zubieta, Solid State Sciences, 4 (2002) 77-82.

[29]   A. Gutierrez, M.F. Perpinan, A.E. Sanchez, M.C. Torralba, M.R. Torres and M.P. Pardo, Inorg. Chim. Acta, 363 (2010) 2443-2451.

[30]   P.D.K. Nezhad, F.V. Azadbakht, H. Amani and R. Khavasi, Acta Crystallogr., Sect. E: Struct. Rep. Online 64 (2008) m575.

[31]   R.A. Machado, M.C. Goite, D. Rivillo, Y. De Sanctis, A.J. Arce, A.J. Deeming, D'Ornelas, L.A. Sierralta, R. Atencio, T. Gonzalez, E. Galarza, J. Organomet. Chem., 692 (2007) 894-902.

[32]   Yu.-Yu. Ng, Ch.-M. Che and Sh.-M. Peng, New J. Chem., 20 (1996) 781-791.

[33]   A. Singh, N. Singh and D. S. Pandey, J. Organomet. Chem., 642 (2002) 48-57.

[34]   H. Grove, N. A. Froystein, L. J. Saethre and J. Sletten, J. Mol. Struct., 800 (2006) 1-17.

[35]   K. Ha, Acta Crystallogr., Sect. E: Struct. Rep. Online, 67 (2011) m1634.

[36]   Ch.-Y. Liao, Ch.-W. Chen, H.-H. Lin, S.-Ch. Cheng, Ch.-J. Lee and H.-H. Wei, J. Chin. Chem. Soc. (Taipei), 52 (2005) 707-716.

[37]   H. Grove, M. Julve, F. Lloret, P.E. Kruger, K.W. Tornroos, J. Sletten, Inorg. Chim. Acta, 325 (2001) 115-124.

[38]   A.B. Wragg, S. Derossi, T.L. Easun, M.W. George, X.-Zh. Sun, F. Hartl, A.H. Shelton, A.J.H.M. Meijer and M.D. Ward, Dalton Trans., (2012) 10354-10371.

[39]   F.S. Delgado, C.A. Jimenez, P. Lorenzo-Luis, J. Pasan, O. Fabelo, C. Delgado, L.F. Lloret, M. Julve and C. Ruiz-Perez, Crystal Growth & Design, 12 (2012) 599-614.

[40]   D.M. D'Alessandro, A.C. Topley, M.S. Davies and F.R. Keene, Chem. Eur. J., 12 (2006) 4873-4884.

[41]   J. Sletten and O. Bjorsvik, Acta Chem. Scand., 52 (1998) 770-777.

[42]   C. Yuste, A. Bentama, S.-E. Stiriba, D. Armentano, G. De Munno, F. Lloret and M. Julve, Dalton Trans., (2007) 5190-5200.

[43]   S.M. Scott, K.C. Gordon and A.K. Burell, J J. Chem. Soc., Dalton Trans., (1999) 2669-2673.

[44]   T. Ishida, T. Kawakami, S. Mitsubori, T. Nogami, K. Yamaguchi and H. Iwamura, J. Chem. Soc., Dalton Trans., (2002) 3177-3186.

[45]   A. Singh, S. K. Singh, M. Trivedi and D. S. Pandey, J. Organomet. Chem., 690 (2005) 4243-4251.

[46]   V. Wing-Wah Yam, V. Wing-Man Lee and K.-K. Cheung, Chem. Commun., (1994) 2075-2076.

[47]   S.W. Magennis, A. Habtemariam, O. Novakova, J.B. Henry, S. Meier, S. Parsons, I.D. H. Oswald, V. Brabec and P.J. Sadler, Inorg. Chem., 46 (2007) 5059-5068.

[48]   Q.-M. Wang and T.C.W. Mak, Inorg. Chem., 42 (2003) 1637-1643.

[49]   K. Ha, Acta Crystallogr., Sect. E: Struct. Rep. Online 68 (2012) m834.

[50]   K. Ha, Acta Crystallogr., Sect. E: Struct. Rep. Online 67 (2011) m1307.

[51]   P. von Grebe, P.J.S. Miguel and B. Lippert, Z. Anorg. Allg. Chem., 638 (2012) 1691-1698.

[52]   K. Ha, Acta Crystallogr., Sect. E: Struct. Rep. Online 68 (2012) m144.

[53]   K. Ha, Acta Crystallogr., Sect. E: Struct. Rep. Online 67 (2011) m1896.

[54]   K. Ha, Acta Crystallogr., Sect. E: Struct. Rep. Online, 67 (2011) m1615.

[55]   D.J. Chesnut, A. Kusnetzow, R.R. Birge and J. Zubieta, Inorg. Chem., 38 (1999) 2663-2671.

[56]   H. Lin, X. Wu and P.A. Maggard, Inorg. Chem., 48 (2009) 11265-11276.

[57]   F. Marandi, A. Marandi, M. Ghadermazi, M. Rafiee and H. Krautscheid, J. Mol. Struct., 1022 (2012) 25-31

[58]   F. Marandi, A. Marandi, M. Ghadermazi, H. Krautscheid and M. Rafiee, J. Coord. Chem., 65 (2012) 1882-1891.

[59]   Y.J. Kim, Y.-A. Lee and O.-S. Jung, Korean journal of crystallography, 11 (2000) 28.

[60]   L. Cunha-Silva, R. Ahmad and M. J. Hardie, Aust. J. Chem., 59 (2006) 40-48.

[61]   Z.-Y. Zhou, Y. Cai, H.-C. Fang, Q.-G. Zhan, H.-J. Jin, Y.-H. Feng and Y.-P. Cai, Inorg. Chim. Acta, 363 (2010) 877-883.

[62]   L. Cunha-Silva, R. Ahmad, M.J. Carr, A. Franken, J.D. Kennedy and M.J. Hardie, Crystal Growth & Design, 7 (2007) 658-667.

[63]   S. H. Park, Y. J. Kim and O.-S. Jung, Bull. Korean Chem. Soc., 23 (2002) 629-632.

[64]   S. Horiuchi, R. Kumai and Y. Tokura, J. Am. Chem. Soc., 135 (2013) 4492-4500.

[65]   A.M. Mădălan, C. Ruiz-pérez, E. Melnic, V. Kravtsov and M. Andruh, Rev. Roum. Chim., 50 (2005) 11-17.

[66]   A. Cucoş, E. Melnic, Yu. A. Simonov and M. Andruh, Rev. Roum. Chim., 54 (2009) 119-125.

[67]   E. Melnic, E.B. Coropceanu, O.V. Kulikova, A.V. Siminel, D. Anderson, H.J. Rivera-Jacquez, A.E. Masunov, M.S. Fonari and V.Ch. Kravtsov, J. Phys. Chem. C, 118 (2014) 30087-30100.

[68]   G.M. Sheldrick, Acta Crystallogr. A, 64 (2008) 112-122.

[69]   C.F. Macrae, P.R. Edgington, P. McCabe, E. Pidcock, G.P. Shields, R. Taylor, M. Towler, J. van de Streek, J. Appl. Crystallogr., 39 (2006) 453-457.

[70]   H.D. Clarke, K.K. Arora, H. Bass, P. Kavuru, T. Teng Ong, T. Pujari, L. Wojtas and M.J. Zaworotko, Crystal Growth & Design, 10 (2010) 2152-2167.

[71]   A.W. Addison, T.N. Rao, J. Reedijk, J. van Rijn and G.C. Verschoor, Journal of the Chemical Society, Dalton Trans., (1984) 1349−1356.

[72]   D.L. Reger, A.E. Pascui, M.D. Smith, J. Jezierska and A. Ozarowski, Inorg. Chem., 51 (2012) 11820−11836.

[73]   A. Pasquarello, I. Petri, P.S. Salmon, O. Parisel, R. Car, É. Tóth, D.H. Powell, H.E. Fischer, L. Helm and A.E. Merbach, Science, 291 (2001) 856−859.

[74] H. Grove, J. Sletten, M. Julve, F. Lloret and L. Lezama, Inorg. Chim. Acta, 310 (2000) 217–226.

[75] H. Lueken, Magnetochemie, Teubner Verlag, Stuttgart, 1999

[76] M. Speldrich, H. Schilder, H. Lueken and P. Kögerler, Isr. J. Chem., 51 (2011) 215–227.

[77] J. Leusen, M. Speldrich, H. Schilder and P. Kögerler, Coord. Chem. Rev., 289–290 (2015) 137–148.

[78] J.S. Griffith, The Theory of Transition-Metal Ions, Cambridge University Press, Cambridge, 1980

Graphical Abstract